Autonomous self commissioning method for speed sensorless controlled induction machines

T.M. Wolbank[1)], M.A. Vogelsberger[1)], R. Stumberger[1)], S. Mohagheghi[2)], T.G. Habetler[2)], R.G. Harley[2)]
1) Department of Electrical Drives and Machines
Vienna University of Technology
Vienna, AUSTRIA
2) School of Electrical and Computer Engineering
Georgia Institute of Technology
Atlanta, GA, USA

Abstract **Speed sensorless control of ac machines at zero speed so far is only possible using signal injection methods. Especially when applied to induction machines the spatial saturation leads to a dependence of the resulting control signals on the flux/load level. Usually this dependence has to be identified on a special test stand during a commissioning procedure for each type of induction machine. In this paper an autonomous commissioning method based on a neural network approach is proposed that does neither depend on a speed sensor present as a reference nor on a load dynamometer coupled to the machine and guaranteeing constant speed. The training data for the neural network is obtained using only acceleration and deceleration measurements of the uncoupled machine. The reliability of the proposed autonomous commissioning method is proven by measurement results. When comparing the resulting sensorless control performance, the proposed commissioning method reaches the same level of performance as a manual identification using load dynamometer as well as speed sensor.**

I. INTRODUCTION

Modern high dynamic ac drives are equipped with a mechanical shaft sensor in order to estimate the flux position, which is required for field oriented or direct torque control. Using fundamental wave models with accurate sensors for voltage and current, the speed sensorless operation of induction machines is possible down to around slip frequency, corresponding to mechanical standstill. However, at zero frequency, the speed sensorless operation is only possible using signal injection methods.

By injecting a high frequency or transient signal in addition to the fundamental wave, saliencies caused by spatial saturation, slotting, and anisotropy can be extracted and exploited to directly estimate the flux/rotor position. The so called signal injection methods usually inject a voltage excitation and measure the current reaction of the machine. The injected signal may be either high frequency harmonic (pulsating or rotating) [1]-[4] or transient (voltage pulses) [5]-[7]. The transient excitation (INFORM method) [5] is used in this paper as sensorless control method. The results however, are applicable to all types of signal injection. The signal obtained from the current response is composed of effects such as inverter and sensor non-linearity as well as the modulations caused by all asymmetries present in the machine that influence the phase leakage parameters. The most prominent of the inherent asymmetries of standard induction machines is that of spatial saturation due to the main flux, followed by the slotting effect and that of rotor anisotropy. Currently, the main problem in the application of speed sensorless control is not the excitation or measurement to obtain the mentioned control signal, but the superposition of all side effects within this signal.

Especially the saturation saliency shows a strong dependence on the flux magnitude as well as the load level of the machine. In addition to the modulations of the three main inherent saliencies, there also exist additional modulations caused by interference of these main effects. This whole interaction and the load/flux dependence of the overall signal denotes the magnetic fingerprint of a machine and depends on parameters like lamination shape, lamination material, winding scheme and slot numbers.

In order to realize satisfactory performance it is therefore necessary to identify this individual behavior for each type of machine during a commissioning phase. In the literature there are already different methods proposed to establish this identification. These are usually based on filtering [3], function approximation or correction tables [9], spatial filtering [10], the so called space modulation profiling [1], or using a neural network based approach [11],[12].

Up to now the commissioning has always been performed using a load dynamometer coupled to the machine and usually also a speed sensor mounted to the shaft as a reference. Thus the identification of the machine's magnetic fingerprint is always a time consuming procedure requiring an expert to be performed. In this paper a new identification method is proposed that is able to perform this task autonomously using only the machine's moment of inertia. Based on a neural network approach the algorithm does neither rely on a speed/ position sensor being present as a reference, nor on a load dynamometer guaranteeing steady state operation during the commissioning. Using only acceleration/deceleration data of the drive, a reliable and accurate detection of the machine specific behavior is performed as will be proven by measurements.

0197-2618/07/$25.00 © 2007 IEEE

II. SENSORLESS CONTROL – MAGNETIC FINGERPRINT

The transient excitation needed for zero speed sensorless control is realized in this paper as a specific voltage pulse sequence applied during inactive operating states of the current control. Measuring the corresponding current step response of the machine and applying the evaluation algorithm [5], [11] leads to a resulting signal that contains all the saliency information of the machine. The sampling rate of the saliency information obtained is 1.25 kHz. As was already investigated and reported by different authors, the magnitude and orientation of the saliencies exhibit a strong dependence on the magnetic point of operation of specific lamination areas (teeth/tips). For speed sensorless control this dependence has thus to be compensated. Currently it is only possible to roughly predict this dependence by simulations based on the design parameters of the machine. This simulation however, is not accurate enough to establish the necessary compensation which raises the need for extensive measurements on a test stand to exactly identify the magnetic fingerprint.

The strongest dependence on the point of operation can be detected on machines with closed rotor slots. Consequently this type of machine has the highest requirements for an accurate identification and compensation with respect to speed sensorless control. Such a closed slot machine has thus been chosen in this investigation to test the performance of the commissioning. To show the mentioned dependence, measurements have been performed and the results are depicted in Fig. 1 for the two main signal components.

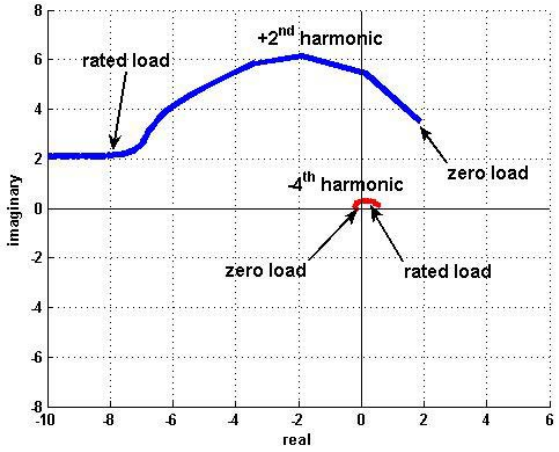

Fig. 1: Load level dependence of the main saturation induced signal components (+2nd blue, -4th red); (locus; internal representation of DSP).

In Fig. 1 the load dependence of the dominant saturation induced components are depicted. The +2nd harmonic is the main harmonic associated with main flux saturation. As shown in the figure there is a very distinct "movement" (magnitude and angle) of this harmonic observable when the load is changed. In addition, the higher order harmonic (-4th) of the saturation saliency changes its orientation leading to a distortion of the resulting signal. Considering only the dependence on the flux level (not shown in the figure), the dominant harmonic is again the +2nd and the biggest distortion is now the –2nd. These have to also be considered during commissioning. It has to be stressed that the locus depicted in the figure is only valid for the specific machine identified (closed slot design – which is considered the most difficult for sensorless control) and may look totally different for machines with other design parameters.

The identification of the main signal components and the removal of the distortion components are key parameters for the speed sensorless control performance. Therefore, the proposed neural network approach offers several advantages compared to the time consuming manual tuning using load dynamometer and a speed sensor as a reference.

III. PROPOSED COMMISSIONING STRUCTURE

The core of the identification process in this paper is a multi layer perceptron (MLP) neural network. Figure 2 illustrates the schematic diagram of the MLP [13]. In its simplest form, a MLP neural network consists of three layers: an input layer, a hidden layer and the output layer. The numbers of neurons in the three layers are denoted by *m*, *n* and *r* respectively. It has been shown in the literature that a three layer MLP is capable of implementing any arbitrary logic function or forming an arbitrarily close approximation to any nonlinear decision boundary or any continuous nonlinear mapping. However, for certain problems the number of nodes in the MLP can be drastically reduced by using two hidden layers rather than one [14].

Each neuron in the hidden layer has a nonlinear activation function Φ associated with it. This function should be bounded, continuous, monotonically increasing and differentiable. Various activation functions have been used in the literature, namely sigmoid, hyperbolic tangent or Gaussian.

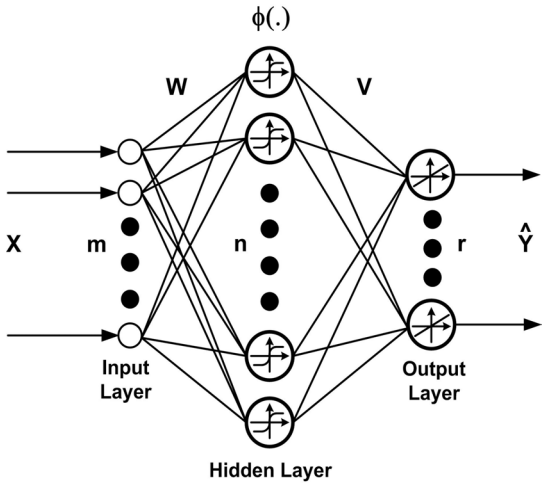

Fig. 2: Schematic diagram of a MLP neural network.

The *m* inputs to each neuron in the hidden layer are weighted with the input weight parameters *W*, summed, and then passed through the activation function Φ. The output of

the neuron, often referred to as the decision vector d, determines whether that specific neuron will fire or hold for a certain set of inputs. The output of the j^{th} neuron in the hidden layer is therefore given by (1):

$$d_j(t) = \Phi[\sum_{i=1}^{m} w_{ji}(t) \times x_i(t)] \cdot \quad (1)$$

The final output of the k^{th} neuron in the output layer of the neural network is then determined from the weighted summation of the outputs of all the individual neurons in the hidden layer, as in (2):

$$\hat{y}_k(t) = \sum_{j=1}^{n} v_{kj}(t) \times d_j(t) \cdot \quad (2)$$

The input weight matrix W and the output weight matrix V can therefore be viewed as the memory cells of the neural network. The training process of the MLP consists of updating these parameters. The most common scheme for training a MLP is backpropagation (BP) algorithm, which has been used through this paper. The basic idea in BP is to form an error function E from the difference between the actual output Y and the estimated output of the neural network $\hat{Y}$:

$$E(t) = \frac{1}{2} \sum_{k=1}^{r} \| y_k(t) - \hat{y}_k(t) \|^2 \quad (3)$$

The weight parameters are then updated in the negative direction of the error gradient:

$$W(t+1) = W(t) - \eta \times \nabla E(t) \,. \quad (4)$$

Similar equation is applied to the output weight matrix V. For detailed information regarding BP the reader is referred to [13].

Even though the number of hidden layers in MLP can be theoretically increased, it is quite often considered to have a single hidden layer. This is to reduce the complexity and the computational effort. Also, for most engineering applications, a single hidden layer seems to be sufficient.

The structure of the MLP identifier used in this paper is illustrated in Fig. 3. It consists of a single hidden layer and a single neuron in the output layer. The number of neurons in the hidden layer is heuristically chosen to be 25.

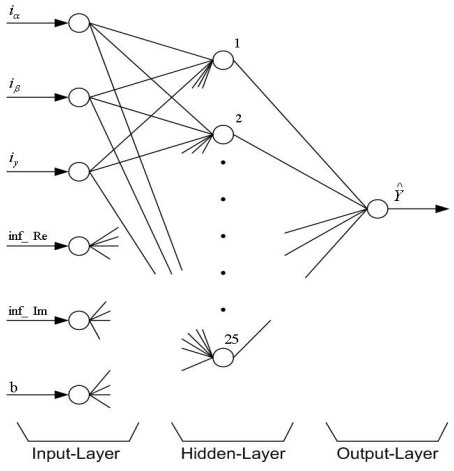

Fig. 3: Input/output structure of the MLP proposed for commissioning.

Increasing the number of neurons in the hidden layer leads to better approximation of the load dependence, however at the same time both the learning performance as well as the execution time of the network is increased. The number of 25 was found to be a good compromise for the specific machine.

The hyperbolic tangent function is used as the activation function of the hidden layer.

$$\Phi(z) = \tanh(z) = \frac{1 - \exp[-z]}{1 + \exp[-z]} \,. \quad (5)$$

The input of the neural network is a m×1 vector $X(t)$ that contains a bias or threshold value (b), which is considered to be 1, plus a number of additional input signals, that contain information on the function to be identified.

The neural network in turn generates an output signal that, after the completion of the training period, is equal to the correction angle. This angle has to be added to the original sensorless control signal obtained from the transient current response in order to eliminate the load dependence and other disturbing effects.

The equation for the output of the neural network is given by (6):

$$\hat{y} = \Phi\left[\left(\sum_{i=1}^{m} W_i \times x_i\right) + 1 \cdot W_{m+1}\right] \quad (6)$$

Compared to directly using the flux angle as output signal, this new configuration has the advantage that there is no need for the network to generate a step every revolution when the angle jumps from $-\pi$ to $+\pi$ (or from 2π to zero).

A. Neural network inputs

The correct selection of the network inputs is one key parameter in the design process to obtain good resulting control performance and at the same time keeping the number of necessary mathematical operations low for real time calculation.

The key parameter to the function to be identified is the torque of the machine which is represented by the two stator current components in the flux fixed reference frame (i_x, i_y). As the machine is usually operated with constant rotor flux in the fundamental speed range, it is sufficient to consider only the torque producing current component (i_y) as input.

The signal to be corrected is the estimated flux angle. In order to be able to also capture disturbance components caused by higher harmonic components of the distribution of the transient leakage along the circumference, this signal is also used as a network input. To avoid the angular steps (2π) every revolution, it is preferred to use the real and imaginary component (inf_{RE}, inf_{IM}) instead.

Basically these three input values should capture the main effects responsible for the angle deviation. However, when realizing such a network structure and looking at the performance of the resulting signal, a considerable deviation is detectable as shown in Fig. 4.

For Fig. 4 the ANN used only the three input signals inf_{RE},

inf_{IM} and i_y. The network was trained using a sensor based model as well as load dynamometer. After the training period the machine was operated at a load torque of 0,8 p.u. . In the upper diagram of Fig. 4 the time traces of the network output (solid, denoted *estimated output*) as well as the reference value (dashed, denoted *reference output*) are shown. All values are scaled in 2π rad. It is clearly visible that the modulation associated with the fundamental wave is correctly tracked by the ANN together with the mean angle deviation associated with the load level.

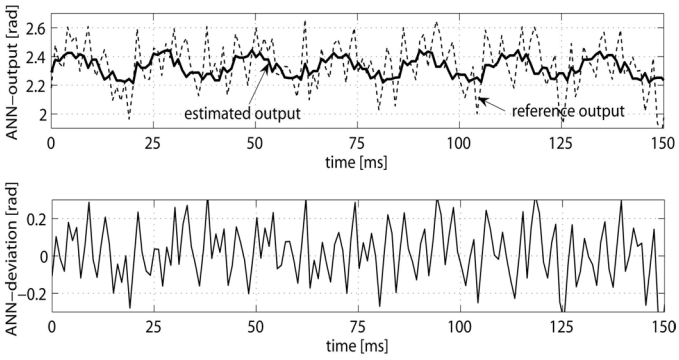

Fig. 4: ANN-Output using inf_{RE}, inf_{IM} and iy as input signals. Upper: ANN-Output (2πrad; solid), reference value of correction angle (2πrad; dashed). Lower: zoomed angle deviation (2πrad).(rated flux, 0,8 load p.u.)

In the lower diagram of Fig. 4 the difference between network output and reference value is given and it clearly shows that the network is not able to track additional modulations not directly correlated to the inputs.

An analysis of this remaining error reveals that this modulation is linked to the angular stator fixed position of the stator current (i_α, i_β).

The reason for this disturbing modulation can be found in deviations of the fundamental wave point of operation due to inverter interlock dead time as well as in the non ideal transfer characteristic of the current sensors during zero crossings [8]. Therefore, a modulation is seen in the deviation signal as a 6th harmonic with respect to the stator fixed reference frame.

To improve the performance of the compensation it is thus necessary to include the two stator fixed current components as network inputs. This structure has been realized and trained as before using a sensor based model as well as load dynamometer.

The corresponding results are given in Fig. 5 where with a load torque of 0.8 p.u the network inputs were as before (Fig. 4) with i_α, i_β added to also track the stator fixed deviations.

The upper diagram in Fig. 5 gives a comparison between the network output (solid) and the reference value that was used for the training period (dashed) scaled in 2π rad. Due to a better approximation the two traces are now almost identical.

In the lower diagram only the difference between the network output and reference value is given to zoom the remaining disturbance. Comparing the lower diagram with that of Fig. 4 it is obvious that the inclusion of the stator fixed values as inputs clearly improves the performance of the disturbance compensation i_α, i_β.

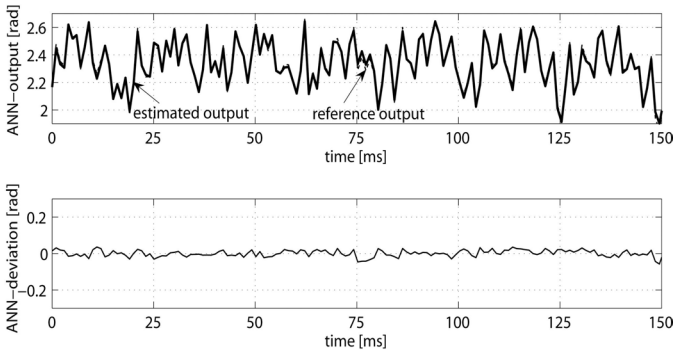

Fig. 5: ANN-Output using inf_{RE}, inf_{IM} and i_y as well as as i_α, i_β as input signals. Upper: ANN-Output (2πrad; solid), reference value of correction angle (2πrad; dashed). Lower: zoomed angle deviation (2πrad).

The estimated output of the network now contains no more correlated components.

It has however, to be stressed that the mentioned stator fixed effects are significant only because the induction machine used for this investigation has closed rotor slots. Using a rotor with semi-closed or open slots, the performance difference between the two input structures would be much smaller.

The network finally used consists of the following input structure:

- a bias or threshold value (b), which is considered to be 1,
- the real and imaginary parts of the stator current (i_α, i_β) in the stator fixed reference frame,
- the torque producing current component (i_y),
- the real and imaginary parts of the sensorless control signal obtained from the current step response (inf_{RE}, inf_{IM}).

After setting up the network structure the training procedure has to be defined to work without a speed sensor as well load dynamometer.

B. Omitting the speed sensor

The training stage of the network is performed using the backpropagation algorithm. During this training (commissioning) a reference value of the rotor flux angle is needed. As no speed/position sensor can be used, a fundamental wave machine model is applied instead. It consists of a modified version of the well known voltage model based on the stator equation of the machine that has some additional feedback loops to reduce the drift of the integrator during low speed operation.

A simplified block diagram of this proposed modified flux model is depicted in Fig. 6 which consists of three main parts.

The dominant one is the block named *Stator Equation* that contains the well known voltage model based on the stator equation. The flux calculation is performed using a pure integrator and not a low pass filter. Inputs to this sensorless structure are the voltage and current space phasors, and the output is the estimated flux space phasor.

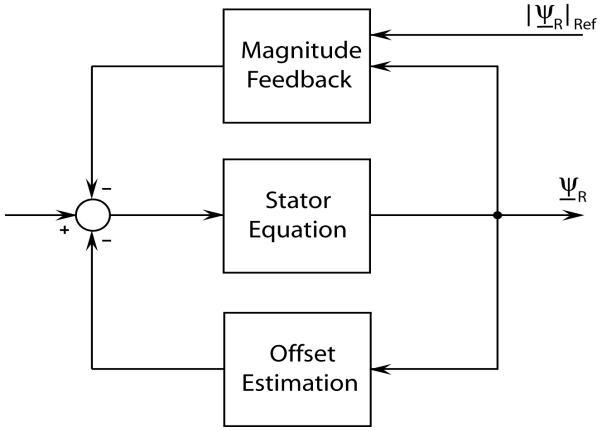

Fig. 6: Structure of the sensorless fundamental wave flux model.

The two remaining blocks, denoted *Magnitude Feedback* and *Offset Estimation*, are used to establish a stabilizing feedback to the integration during low speed operation.

For the flux magnitude comparison the rated flux value (1.0 p.u.) is used as the machine is operated with constant flux at low speed.

After correctly identifying the machine parameters with an adaptation algorithm not shown in Fig. 6, the structure guarantees stable operation down to a few percent of rated speed.

As sensorless operation cannot be achieved using the fundamental wave model only, the commissioning has to be done at higher frequencies where the modified voltage model delivers a reliable estimate of the actual rotor flux position that can be used as a reference value.

There is, however, also an upper frequency limit, that should not be exceeded during the training of the network. It is determined by two effects:

- One is the modulation index of the PWM scheme that impedes the placing of the necessary test voltage sequence when approaching over modulation, and the other is the
- field weakening range that has to be avoided in order to ensure constant main flux level during the training phase.

The inclusion of the flux level dependence would not bring an advantage for the speed sensorless control, but only drastically increase the complexity of the network itself as well as for the training and the compensation afterwards.

C. Omitting the load dynamometer

The main operating parameter for the identification is thus the machine torque (torque producing current component, see also Fig. 3). If a load dynamometer was coupled to the test machine then the commissioning would be done at a constant and well defined frequency and all data obtained could be directly applied to the training algorithm.

However, as the goal is to perform the training without a load dynamometer, the speed of the drive is not going to be constant. As a consequence the machine speed will thus change depending on the load current as well as the moment of inertia.

The training data are thus obtained by repeatedly accelerating and decelerating the machine between two frequency limits. The lower limit is determined by the accuracy of the fundamental wave model and the upper limit by the modulation index of the PWM.

The training procedure is depicted in Fig. 7. The upper diagram of the figure gives the machine speed during that phase. The machine is repeatedly accelerated and decelerated between the two frequency limits which have been chosen as 0.15 p.u. and 0.3 p.u. to ensure enough distance from the actual limits.

The lower diagram gives the time trace of the reference (black) and actual (gray) value of the load current. After each acceleration/deceleration cycle the load current is increased stepwise.

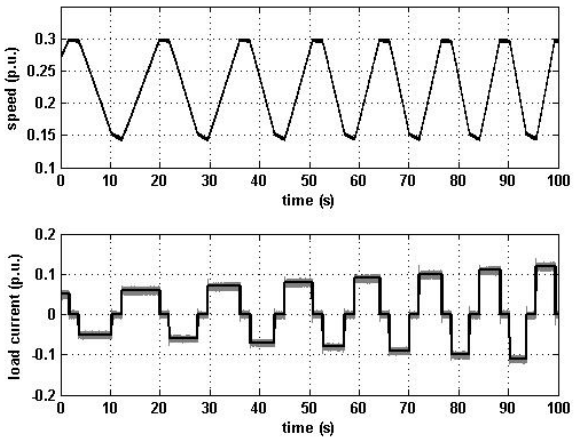

Fig. 7: Training of the proposed structure. Upper: speed (p.u.); Lower: actual (gray) and reference (black) load current.

However, this commissioning during transient speed operation however implies an accurate knowledge of the corresponding speed during the transient changes.

The saliencies present in the machine do not depend on the machine frequency. However, as the pulse sequence, current sampling, as well as the evaluation algorithm need some time to be performed, the whole sampling/signal processing introduces a dead time that leads to a frequency dependent angle delay. To compensate for this delay an accurate estimation of the current frequency with zero delay is necessary.

This is achieved by combining prediction and interpolation methods which can be applied as the machine is only loaded by the constant moment of inertia. The reference values for the prediction/interpolation of the frequency are determined during the short periods of no load condition. Thus a set of training data is obtained.

Two additional effects have to be taken into account before feeding the data to the training algorithm:

- Due to the constant frequency limits the time needed for each acceleration cycle decreases with increasing torque.

Assuming constant sample frequency of the pulse injection method, this would lead to a reduction of the number of reference values with increasing torque level. As a consequence the accuracy of the network at lower torque levels would be increased and at the same time that at higher torque levels reduced. To avoid this effect it has to be assured that the overall number of samples taken for each load level does not change significantly.

- To also ensure an equal distribution of all sampled values over the full angular range (+/-π) it is necessary to perform some post processing of the samples by segmenting as well as by always using an integer number of revolutions.

After applying the above considerations, the training is done using the well known backpropagation algorithm.

IV. Measurement Results

After the autonomous training stage, measurements were performed under speed sensorless operation using the signal obtained from the transient current response combined with the sensorless fundamental wave model used during the commissioning phase (Fig. 6).

The resulting performance can be seen in the following figures. The machine used for the tests has closed rotor slots which results in a heavy load dependence and needs a very accurate compensation.

In Fig. 8 the machine was operated at 0.8 p.u. rated torque, with a speed controlled load dynamometer coupled to it. The upper diagram in the figure gives the time trace of the flux angle obtained from the transient current response, corrected by the output of the neural network, and filtered by the fundamental wave model. At the left side of the figure the mechanical speed was chosen to zero. In the center of the figure the operation was changed to zero flux frequency and on the right side of the figure again zero mechanical speed is shown. The proposed commissioning is therefore able to autonomously "learn" the heavy load dependence of the closed rotor slot machine.

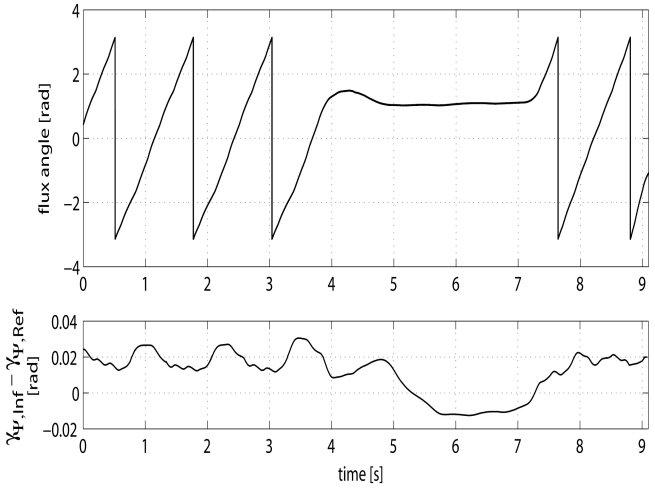

Fig. 8: Low/zero speed performance of proposed compensation at 0,8 p.u. rated torque. Upper: flux angle sensorless (2πrad), Lower: angle deviation (2πrad).

The lower diagram of Fig. 8 depicts the angle deviation between the sensorless estimated flux angle and the flux angle calculated by a sensor based model as a reference.

In this zoomed representation it can be seen that the angle deviation during the zero speed as well as the zero frequency operation, is extremely low.

The performance during a torque step response is depicted in Fig. 9. There a torque step is forced into the sensorless controlled test machine while it is driven on a test stand by a speed controlled load machine. The mechanical speed is almost standstill when the step for the torque demand is made from 0.45 p.u. to 0.8 p.u.

In the upper diagram of Fig. 9 the solid trace represents the time trace of the flux angle obtained from the transient current response, corrected by the output of the neural network, and filtered by the fundamental wave model. The dashed trace gives the reference flux angle calculated with a sensor based model as a reference. The middle part of Fig. 9 shows the load current/torque steps up and down. In the lower diagram of this figure the angle deviation is shown.

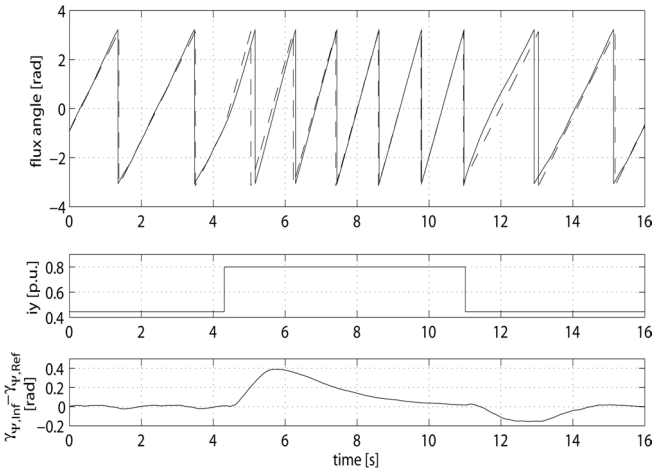

Fig. 9: Measurement results of sensorless controlled operation around mechanical standstill - step of the load torque from 0,45p.u. to 0.8p.u. rated load current/torque. Upper: flux angle sensorless (solid), sensor based (dashed). Middle: load current/torque step. Lower: angle deviation (2πrad)

The transient increase of the angle deviation after the load step is applied is mainly caused by an incorrect dynamic estimation of the stator frequency. This however, does not deteriorate the performance of the commissioning procedure proposed in this investigation.

V. Conclusions

A structure for self commissioning of speed sensorless control has been proposed. It is able to work without shaft sensor as a reference as well as without a load dynamometer coupled. The proposed structure is based on a multilayer perceptron, a modified voltage model, as well as a high dynamic frequency determination. It is able to obtain the needed training samples from acceleration/deceleration measurement. After commissioning, sensorless operation on a closed rotor slot induction machine was proven possible at

high torque levels at low as well as zero speed/frequency.

ACKNOWLEDGMENT

The authors gratefully acknowledge the financial support of the Austrian Science Foundation - "Fonds zur Förderung der wissenschaftlichen Forschung" (FWF) - under grant no. P19967-N14.

REFERENCES

[1] C. Caruana, G.M. Asher and K.J. Bradley and M. Woolfson, "Flux Position Estimation in Cage Induction Machines Using Synchronous Hf Injection and Kalman Filtering", in Proc. *IEEE IAS*, Pittsburgh, PA, USA, pp. 845-850, (2002).

[2] A. Consoli, "Machine Sensorless Control Techniques Based on HF Signal Injection", in Proc. *EPE-PEMC*, V1, pp. 98-103, (2000).

[3] M.W. Degner and R.D. Lorenz, "Using Multiple Saliencies for the Estimation of Flux, Position, and Velocity in AC Machines", in Proc. *IEEE IAS,* New Orleans, LA, USA, pp. 760-767, (1997).

[4] J.I. Ha and S.K. Sul, "Physical Understanding of High Frequency Injection Method to Sensorless Drives of an Induction Machine", in Proc. *IEEE IAS*, pp. 1802-1808, (2000).

[5] M. Schroedl, "Sensorless Control of AC Machines at Low Speed and Standstill based on the Inform Method", in Proc. *IEEE IAS*, vol.1, pp. 270-277, (1996).

[6] C. Caruana, G.M. Asher and J. Claire, "Sensorless Vector Control at Low and Zero Frequency Considering Zero-Sequence Current in DeltaConnected Cage Induction Motors", in Proc. *IEEE IECON*, pp. 1460-1465, (2003).

[7] J. Holtz J, "Sensorless Position Control of Induction Motors–an Emerging Technology", in Proc. *IEEE AMC,* pp. 1-14, (1998).

[8] Th.M. Wolbank and J.L. Machl, "Influence of Inverter Non-linearity and Measurement Setup on Zero Speed Sensorless Control of AC Machines Based on Voltage Pulse Injection", in Proc. *IEEE IECON,* Raleigh, NC, USA, pp. 1568-1573, (2005).

[9] F. Briz, M.W. Degner, A. Diez and R.D. Lorenz, "Measuring, Modeling and Decoupling of Saturation-Induced Saliencies in Carrier Signal Injection-Based Sensorless AC Drives", in Proc. *IEEE IAS*, vol. 3, pp. 1842-1849, (2000).

[10] J. Holtz and H. Pan, "Elimination of Saturation Effects in Sensorless Position Controlled Induction Motors", in Proc. *IEEE IAS*, vol.3, pp.1695-1702, (2002).

[11] Th.M. Wolbank, J.L. Machl and Th. Jaeger, "Combination of Signal Injection and Neural Networks for Sensorless Control of Inverter Fed Induction Machines", in Proc. *IEEE PESC*, Aachen, Germany, pp. 2300-2305, (2004).

[12] P.Garcia, F.Briz, D.Raca and R.Lorenz, "Saliency tracking-based, sensorless control of ac machines using structured neural networks", in Proc. *IEEE IAS*, pp. 319-326, (2005).

[13] S.S. Haykin, *Neural Networks: A Comprehensive Foundation,* Prentice Hall, 2nd Edition, (1998), ISBN 0-1327-3350-1.

[14] D.R. Hush and B.G. Horne, "Progress in Supervised Neural Networks", *IEEE Signal Processing Magazine*, pp 8-39, January (1993).